

Solid-State  $^{17}\text{O}$  NMR of Amino Acids

K. J. Pike,<sup>†</sup> V. Lemaitre,<sup>‡,§</sup> A. Kukol,<sup>||</sup> T. Anupöld,<sup>⊥</sup> A. Samoson,<sup>⊥</sup> A. P. Howes,<sup>†</sup> A. Watts,<sup>‡</sup> M. E. Smith,<sup>\*,†</sup> and R. Dupree<sup>\*,†</sup>

Departments of Physics and Biological Sciences, University of Warwick, Coventry CV4 7AL, U.K., Biosciences Department, Nestlé Research Centre, Vers-chez-les-Blancs, P.O. Box 44, CH-1000 Lausanne 26, Switzerland, Biochemistry Department, University of Oxford, South Parks Road, Oxford OX1 3QU, U.K., and National Institute for Chemical Physics and Biophysics, Akadeemia Tee 23, Tallinn, Estonia

Received: January 5, 2004; In Final Form: April 20, 2004

$^{17}\text{O}$  solid-state NMR from 14 amino acids is reported here, greatly increasing the number investigated. In most cases well-separated resonances from carbonyl and hydroxyl oxygens with distinct second-order quadrupolar line shapes are observed using a 600 MHz spectrometer with fast magic angle spinning (MAS). This is in contrast to the motionally averaged resonances usually seen from amino acids in solution. For amino acids double-angle rotation (DOR) produces a decrease in the line width by more than a factor of 40, providing very high resolution,  $\sim 1$  ppm, spectra. The oxygen lines in alanine and the carbonyl oxygens in L-glutamic acid hydrochloride are assigned using  $^1\text{H}$ -decoupled DOR. The NMR interaction parameters for amino acids show a wide variation of  $\chi_Q$ , from 6.4 to 8.6 MHz,  $\eta$ , from 0.0 to 0.9, and  $\delta_{\text{iso}}$ , from 83 to 353 ppm. The high quality of the MAS NMR line shapes obtained at 14.1 T means that even small changes in parameters can be very accurately deduced, offering the possibility of  $^{17}\text{O}$  NMR as a sensitive probe of structural changes in these and related compounds. The D- and L-forms of glutamic acid hydrochloride are shown to have the same NMR parameters to within error, which are very different from those reported in the literature for the D,L-form. A strong correlation ( $\sim -1200$  ppm/Å) is found between  $\delta_{\text{iso}}$  and the C–O bond length of the carbonyl oxygens. On the basis of these data, enriching specific amino acids in more complex polypeptides and proteins could provide site-selective information about the bonding and functionality of different sites in biomolecules. An estimate is made of the possible detection limit for such species.

## Introduction

The widespread occurrence of oxygen in many technologically and scientifically interesting materials would suggest that NMR studies of this nucleus could provide much crucial information about the structure and bonding in a wide range of materials. However, the spin  $I = 5/2$  nucleus  $^{17}\text{O}$  with a natural abundance of 0.037% is the only NMR-active isotope of oxygen, and as it possesses a quadrupole moment,  $^{17}\text{O}$  resonances are often significantly broadened in solids.<sup>1</sup> It is the combination of low sensitivity and sometimes large line widths that make  $^{17}\text{O}$  NMR studies still relatively uncommon. However, there is high sensitivity of the NMR parameters such as the isotropic chemical shift (covering  $\sim 1000$  ppm in organic molecules) and the quadrupole parameters to structural detail. Study of oxygen has been further encouraged by the advent of higher magnetic fields, faster magic angle spinning (MAS), and techniques for improving resolution<sup>1</sup> (e.g., dynamic angle spinning (DAS), double-angle rotation (DOR), multiple-quantum (MQ) MAS). This has led to a significant increase in  $^{17}\text{O}$  NMR reports from inorganic materials<sup>2</sup> with examples of  $^{17}\text{O}$  NMR studies of amorphous materials to determine nanoscale phase separation in silica-based gels<sup>3–5</sup> and the distribution of bonding species

in a range of glasses.<sup>6–9</sup> There have also been studies of crystalline materials such as zeolites and mineral analogues,<sup>10–13</sup> but with much less work on organic materials since the powder line shapes are typically much broader because of the large electric field gradient as a result of the increased covalency of the M–O bonds in these materials.

A key experimental challenge for biomolecular chemistry is to provide high-quality, detailed, and unambiguous atomic-scale information about the molecular bonding arrangement and changes that occur upon ligand–receptor interaction. Solid-state NMR is one nonperturbing approach which can be used to study such interactions where molecular size is not limiting and crystallinity not a requirement,<sup>14,15</sup> and the ubiquity of oxygen throughout living systems should imply that  $^{17}\text{O}$  is an important nucleus for such studies. Oxygen plays a key role in intra- and intermolecular interactions, with hydrogen-bonding important in biological processes so that  $^{17}\text{O}$  could provide detailed information about the dynamics and structure of amino acids both in the solid state and in solution. This demands the development of experimental probe techniques to deliver this information.  $^{17}\text{O}$  NMR from inorganic materials such as that cited above has shown that the sensitivity of the NMR parameters to structural detail gives great encouragement for the NMR study of organic materials. Recent reports of high-field  $^{17}\text{O}$  NMR from organic materials have included heme proteins,<sup>16</sup> strongly hydrogen-bonded carboxylic acids,<sup>17</sup> nucleic acid bases,<sup>18</sup> and other organic materials.<sup>19</sup>

In proteins it is important to understand processes such as folding, which is related to functional properties and disease,

\* To whom correspondence should be addressed. E-mail: R.Dupree@warwick.ac.uk (R.D.); M.E.Smith.1@warwick.ac.uk (M.E.S.).

<sup>†</sup> Department of Physics, University of Warwick.

<sup>‡</sup> Nestlé Research Centre.

<sup>§</sup> University of Oxford.

<sup>||</sup> Department of Biological Sciences, University of Warwick.

<sup>⊥</sup> National Institute for Chemical Physics and Biophysics.

in terms of the conformation through the secondary structure. It is the amino acid sequence and the interresidue bonding that influence this structure. The more common nuclei for the NMR study of such problems are  $^1\text{H}$ ,  $^{13}\text{C}$ , and  $^{15}\text{N}$ .  $^{17}\text{O}$  would be another possible NMR approach, with the potential importance of  $^{17}\text{O}$  being recognized through attempts more than 20 years ago to obtain  $^{17}\text{O}$  NMR spectra from amino acids and peptides in solution. The work of Fiat and co-workers presented detailed  $^{17}\text{O}$  enrichment protocols, most often specifically labeling the carbonyl site. The solution spectra from a series of [ $^{17}\text{O}$ ]-carbonyl-exchanged amino acids gave single intense carbonyl resonances typically between 249 and 265 ppm.<sup>20,21</sup> Spectra from solids are potentially more informative than those from solution as both the shift and the quadrupole coupling constant  $\chi_Q$  (with  $\chi_Q = e^2Qq/(2I(2I - 1)h)$ ;  $eQ$  is the quadrupole moment and  $eq$  is the maximum component of the electric field gradient) and the asymmetry parameter  $\eta$  can be determined. Furthermore, different sites are not averaged to single resonances by motion and/or exchange that is present in solution. Often the solid state is more representative of the natural bonding state (e.g., in a membrane) than a solution. Also knowledge of the interaction parameters aids interpretation of the solution spectra (e.g., if  $\chi_Q$  is known, NMR provides the correlation time more unambiguously). Hence, extension to the solid quickly followed the initial solution-state studies.<sup>22,23</sup> However, there were a number of factors that counted against the ability to obtain the high-quality NMR spectra which would allow NMR parameters to be unambiguously determined including low applied magnetic field (e.g., 6.35 T), initially no MAS, and then only modest MAS rates. The second-order quadrupole powder patterns that were obtained often showed significant distortion from the true line shapes with, for example, narrow spectral features such as the singularities often disproportionately intense. Static NMR had the added disadvantage that the line shape contains both second-order quadrupole and chemical shift anisotropy (CSA) effects so that it was difficult to unambiguously determine the interaction parameters. The problems with simulation and excitation of this early  $^{17}\text{O}$  NMR work can be gauged by values of  $\chi_Q$  as low as 4 MHz being reported for polyglycine II compared with a true value of 8.2 MHz.<sup>24,25</sup>

In recent years the situation has rapidly improved with the more widespread availability for solid-state NMR studies of magnetic fields of  $\geq 14.1$  T and MAS rates of  $>25$  kHz. Work compared four [ $^{17}\text{O}$ ]carbonyl-labeled polyglycines which show very different hydrogen-bonding with variations of 8.30–8.55 MHz in  $\chi_Q$ , 0.26–0.47 in  $\eta$ , and 288–407 ppm in the isotropic chemical shift ( $\delta_{\text{cs,iso}}$ ).<sup>25</sup> The richness of the solid-state data over those from solution where there is much less variation in the bonding and there are averaging effects is illustrated by a shift variation of  $\sim 120$  ppm from these compounds compared to the report of a single shift of 267 ppm in solution.<sup>25</sup> This shift variation is also much greater than those reported for  $^{13}\text{C}$  and  $^{15}\text{N}$  from the same compounds. The variation in these parameters between polyglycines I and II is related to differences in the molecular packing between the  $\beta$ -sheet and  $3_1$ -helix forms.<sup>26</sup> A  $^1\text{H}$ – $^{17}\text{O}$  double-resonance NQR study of polycrystalline D,L-proline showed eight different signals that were found to fall into two groups that could be assigned to hydroxyl ( $\chi_Q = 6.08$ – $6.79$  MHz) and carbonyl ( $\chi_Q = 7.72$ – $8.73$  MHz) oxygens.<sup>27</sup> This assignment could be made on the basis of the relative values of  $\chi_Q$  and because in the  $^1\text{H}$ – $^{17}\text{O}$  double-resonance approach the signal assigned to the hydroxyls shows a much stronger enhancement. Two poly(L-alanines) which adopted the  $\alpha$ -helix and  $\beta$ -sheet forms were readily distinguished through

the different  $\chi_Q$  and  $\delta_{\text{cs,iso}}$  values of the enriched carbonyl sites.<sup>28</sup> A two-field DAS study of a uniformly  $^{17}\text{O}$  labeled sample of the parent amino acid L-alanine showed two completely resolved  $^{17}\text{O}$  signals, with the position of the lines at 11.7 T differing by 29 ppm. High-power  $^1\text{H}$  decoupling substantially narrowed the DAS lines.<sup>29</sup> The two signals arise from distinct sites in the structure, with O(1) the conventional hydrogen bond with  $\text{O}\cdots\text{N}$ , whereas the other oxygen, O(2), site is bifurcated as the attached proton is also connected to two other nitrogens. In D-alanine a 3Q MAS study was carried out with again two sites observed.<sup>30</sup> These two studies gave reasonable agreement between the shifts of the two sites, and for one site  $P_Q = \chi_Q(1 + \eta^2/3)^{1/2}$  also agreed within error. However, for the other site the values for  $P_Q$  from the two studies did not agree within error, and this will be examined in this paper.  $^{17}\text{O}$  NMR of tyrosine hydrochloride labeled at the phenyl OH (i.e., not at the COOH) position gave a shift more than 150 ppm smaller than that of either site in alanine with a much larger  $\chi_Q$ . Comparison of static and MAS NMR spectra indicated that there was a CSA of  $\sim 100$  ppm.<sup>19</sup> Recently, we reported a detailed  $^{17}\text{O}$  NMR study of the L-form of glutamic acid hydrochloride<sup>31</sup> which gave NMR parameters very different from those of some of the sites reported for the D,L-form.<sup>30</sup> The D,L-form of glutamic acid showed a resonance additional to those of the pure L-form with  $\sim 50\%$  of the total intensity, which implies that D,L-glutamic acid is a racemic crystal as opposed to a racemic conglomerate of chiral crystals.<sup>30</sup>

Despite this initial work on  $^{17}\text{O}$  in amino acids, there is still no detailed knowledge of the range of values the NMR interaction parameters take (especially of C–OH) nor the relationship these parameters have to structure. It has been suggested that  $\chi_Q$  has a linear relationship to the  $\text{N}\cdots\text{O}$  bond length.<sup>26</sup> However, a recent computational study using density functional theory calculated the NMR interaction parameters from  $\alpha$ -helix and  $\beta$ -sheet conformations and suggested there was no dependence on the bond length.<sup>32</sup> Distinct quadrupolar parameters from each of these conformations were calculated with  $\chi_Q$  changing by 0.53 MHz, much larger than the accuracy with which it can be determined. The variations come from differences in the hydrogen bond and backbone dihedral angles, thus solid state  $^{17}\text{O}$  NMR approach offers much potential for understanding subtle variations in the local bonding. In this paper we seek to extend the understanding of the utility of  $^{17}\text{O}$  by greatly increasing the number of  $^{17}\text{O}$  parameters from amino acids, reporting the NMR parameters of 14 amino acid samples.

## Experimental Details

Amino acids were  $^{17}\text{O}$ -enriched using either a slight variant of the procedure described previously for  $^{18}\text{O}$  enrichment<sup>33</sup> or that described previously by us for enriching L-glutamic acid.<sup>20,31</sup> In brief, the amino acid was suspended in a mixture of  $^{17}\text{O}$ -enriched water and dioxane (1:3, v/v). Water was used in 25-fold molar excess over the amino acid. The mixture was treated with a continuous stream of HCl gas obtained from  $\text{MgCl}_2/\text{H}_2\text{SO}_4$  for 2 h while being kept at 90 °C. The sample was lyophilized and the  $\text{H}_2^{17}\text{O}$ /dioxane recovered. Water enriched to 10–20 atom %  $\text{H}_2^{17}\text{O}$  was found to be sufficient to achieve an acceptable signal-to-noise (S/N) ratio for the solid-state NMR spectroscopy of these simple amino acids. The HCl form of the amino acid is produced using this enrichment route. [ $^{17}\text{O}_2$ ]-L-Alanine hydrochloride was prepared by acid-catalyzed exchange with  $\text{H}_2^{17}\text{O}$  following literature procedures.<sup>20,30</sup> A 900 mg sample of L-alanine was dissolved in 1 g of  $\text{H}_2^{17}\text{O}$  in a 3.0 mL glass vial. The solution was saturated with dry HCl gas,

sealed, and then heated to 100 °C for approximately 24 h. The sample was then cooled to room temperature and allowed to crystallize, followed by several successive recrystallizations in the  $\text{H}_2^{17}\text{O}$  used for the exchange. Finally, the sample was cooled to 4 °C, and crystals were recovered.  $\text{H}_2^{17}\text{O}$  was recovered using microdistillation under a  $\text{N}_2$  atmosphere.  $[\text{O}_2^{17}\text{O}]$ -L-Alanine was prepared using a similar procedure with less alanine (800 mg), more water (2 g), and only partial saturation with HCl. The initial amino acids were all supplied at >99.8% purity followed by straightforward processing by placing them in water and passing HCl gas, which should not change the form of the amino acid present other than producing  $^{17}\text{O}$  enrichment and the HCl salt. The identity of the product was confirmed by solid-state  $^{13}\text{C}$  NMR and powder XRD.  $^{13}\text{C}$  NMR was performed on a Chemagnetics Infinity 600 or 360 spectrometers operating at 150.92 and 90.55 MHz, respectively. A 4 mm probe was used spinning at 7.5–10 kHz with contact times of 1 ms. Powder XRD was run on a Bruker D5005 diffractometer using  $\text{Cu K}\alpha_1$  radiation at a wavelength of 1.5405 Å. The patterns were taken from  $2\theta = 10^\circ$  to  $2\theta = 90^\circ$  in  $0.2^\circ$  steps, spending 4–8 s at each point. Both  $^{13}\text{C}$  and powder XRD confirmed the samples were as expected and were single phase. On some samples  $^{35}\text{Cl}$  NMR was also used as further confirmation.

Most of the  $^{17}\text{O}$  NMR was carried out on a Chemagnetics Infinity 600 spectrometer at a frequency of 81.345 MHz. MAS and 3Q MAS experiments used either a 4 mm probe spinning at ~16 kHz or a 3.2 mm MAS probe spinning at 17–22 kHz. The recycle delay was typically 3 s, which was sufficient to prevent saturation. Typically, ~20K scans were sufficient to give an adequate S/N ratio with the 3.2 mm probe for samples produced from 20%  $^{17}\text{O}$  enriched water. A spin echo using extended phase cycling<sup>34</sup> was used with the echo spacing set to the rotation period. High-power  $^1\text{H}$  decoupling using the XiX scheme<sup>35</sup> was employed where necessary. It was very important to be exactly on angle as the combination of the echo and  $^1\text{H}$  decoupling produced very high quality second-order quadrupolar line shapes. Even small deviations from the angle significantly affected the NMR parameters deduced from the line shape. Experiments using DOR NMR were carried out using odd-order sideband suppression where the acquisition of successive scans is triggered at orientations of the outer rotor differing by  $180^\circ$ .<sup>36</sup> The outer rotor speed was varied between 1300 and 1800 Hz to determine the centerbands. Again a recycle delay of typically 3 s was required, but the very much narrower resonance lines meant that only ~2000 scans were needed. The DOR probe, which was constructed in one of our laboratories, also has the facility for simultaneous  $^1\text{H}$  irradiation, and in some cases spectra were acquired with a range of decoupling fields up to 34 kHz. All spectra were referenced to water at 0 ppm. Some additional spectra were acquired at a magnetic field of 8.45 T and a frequency of 48.8 MHz. Spectral simulations were carried out using the dmfit software.<sup>37</sup>

## Results

Examples of typical  $^{17}\text{O}$  MAS NMR spectra from amino acids are shown in Figure 1 from L-tyrosine hydrochloride (a), L-asparagine hydrochloride (b), L-valine hydrochloride (c), and L-glycine hydrochloride (d). In these samples which are uniformly labeled in the COOH group, there are two well-separated resonances, both with distinct second-order quadrupole line shapes. Also shown in Figure 1 are simulations which are of high accuracy because of the clear separation of the lines and the well-delineated line shapes, with the parameters deduced summarized in Table 1. The two lines are from the carbonyl

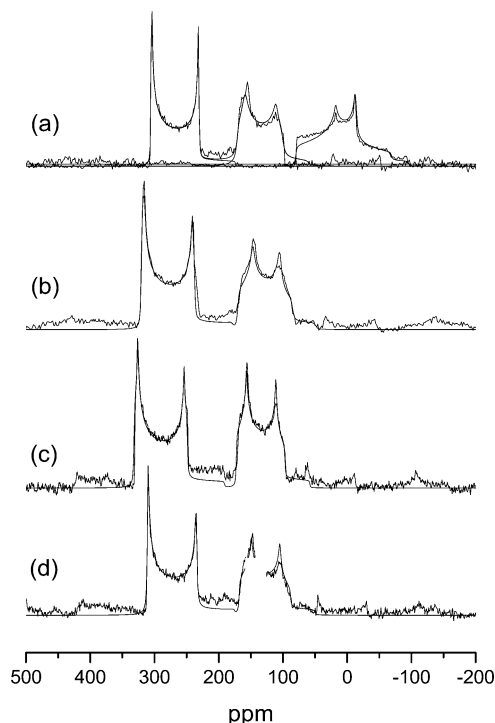


**Figure 1.**  $^{17}\text{O}$  MAS NMR (14.1 T) spectra of (a) L-tyrosine hydrochloride, (b) L-asparagine hydrochloride, (c) L-valine hydrochloride, and (d) L-glycine hydrochloride together with simulations of the centerbands. (Note the L-tyrosine spectrum is a composite of two samples, one  $^{17}\text{O}$ -enriched in the two oxygens of the carboxylate group and the other in the phenol position.)

and hydroxyl oxygens, with the higher shift line from the carbonyl. This assignment is justified by comparison with the shifts observed from carbonyls and hydroxyls in solution. Also the  $^{17}\text{O}$  resonances from solid poly(amino) acids selectively enriched at the carbonyl site typically have  $\chi_Q \approx 8.2$  MHz and  $\delta_{\text{cs,iso}} \approx 300$  ppm, further confirming this assignment. The spectrum of a L-tyrosine sample selectively enriched at the hydroxyl group attached to the phenol group (Cambridge Isotope Laboratories) is also shown in Figure 1a; it is much sharper than that previously reported,<sup>30</sup> allowing a more accurate determination of the parameters. The values of  $\chi_Q$  (8.56 MHz) and  $\eta$  (0.65) are much higher than those of the hydroxyl in the COOH group (7.35 MHz, 0.19), and the shift is 100 ppm less.

The spectra of the other two oxygen site amino acid hydrochlorides are similar to those in Figure 1, and their NMR parameters are given in Table 1, which has representatives of all the main classes of amino acids, nonpolar, polar, acidic, and basic. The sensitivity of the  $^{17}\text{O}$  NMR parameters is well illustrated by a sample of valine that was initially  $^{17}\text{O}$ -enriched and then subsequently reacted with 9-fluorenylmethoxycarbonyl (fmoc) to protect the oxygen-labeled sites during further synthesis. The  $^{17}\text{O}$  MAS NMR spectrum again shows two clearly separated second-order quadrupolar line shapes, from the carbonyl and hydroxyl oxygens, but their parameters are significantly different from those of pure valine (Table 1).

Figure 2a shows the spectrum of L-alanine hydrochloride, together with a simulation, which is similar to those of the other acid hydrochlorides with clearly resolved C=O and OH lines. The spectrum of L-alanine shown in Figure 2b is very different from that obtained for L-alanine hydrochloride and from the typical spectra of the other amino acid hydrochlorides. The two strongly overlapping lines lie between those of L-alanine hydrochloride, but sufficient features can be resolved to allow a good simulation. To confirm and further refine the parameters

TABLE 1:  $^{17}\text{O}$  NMR Interaction Parameters for Amino Acids

compd, line	$\delta_{\text{cs,iso}} \pm 0.5$ ppm	$\chi_{\text{Q}} \pm 0.05$ MHz	$\eta \pm 0.02$	assignment	ref	structure ref
L-glutamic acid hydrochloride						
1	322.0	8.16	$0.0 \pm 0.03$	O2	31	43
2	315.0	8.31	0.17	O3		
3	187.0	7.49	0.25	O1 or O4		
4	172.5	7.45	0.25	O1 or O4		
D-glutamic acid hydrochloride					this study	
	322.0	8.22	$0.03 \pm 0.03$	O2		
	315.4	8.35	0.17	O3		
	187.2	7.49	0.25	O1 or O4		
	172.3	7.45	0.25	O1 or O4		
D,L-glutamic acid hydrochloride					30	na <sup>b</sup>
1	320	8.2	0.0			
2	250	6.8	0.58			
3	250	6.8	0.58			
4	170	7.2	0.20			
D-alanine					30	
1	$275 \pm 5$	$7.60 \pm 0.02$	$0.60 \pm 0.01$	O1		
2	$262 \pm 5$	$6.40 \pm 0.02$	$0.65 \pm 0.01$	O2		
L-alanine					28	42
1	$285 \pm 8$	$8.1 \pm 0.3^a$		O1		
2	$268 \pm 8$	$7.2 \pm 0.3^a$		O2		
L-alanine					this study	42
1	284	7.86	0.28	O1		
2	260.5	6.53	0.70	O2		
L-alanine hydrochloride						49
	327.8	8.31	0.0	C=O		
	176.7	7.29	0.20	OH		
fmoc-protected alanine					this study	
1	303.3	7.89	0.16			
2	175.7	6.95	0.12			
glycine hydrochloride					this study	49
1	336	8.40	0.0	C=O		
2	185	7.60	0.25	OH		
L-tyrosine hydrochloride					this study	50
1	327.0	8.22	0.0	C=O		
2	183.0	7.35	0.19	OH		
3	83	8.56	0.65	O3 (OH)		
D,L-tyrosine hydrochloride					30	
3	117	8.1	1.0	OH		
asparagine hydrochloride					this study	na
1	342.5	8.55	0.00	C=O		
2	178.5	7.49	0.30	OH		
valine hydrochloride					this study	51
1	351	8.40	0.03	C=O		
2	181	7.35	0.21	OH		
fmoc-protected valine					this study	
1	324.1	8.42	0.08			
2	167.3	7.48	0.27			
leucine hydrochloride					this study	na
1	342.7	8.39	0.05	C=O		
2	183.1	7.50	0.20	OH		
isoleucine hydrochloride					this study	na
1	347.1	8.52	0.06	C=O		
2	182.6	7.40	0.22	OH		
lysine hydrochloride					this study	na
1	346.7	8.56	0.0	C=O		
2	180.8	7.67	0.24	OH		
phenylalanine hydrochloride					this study	52
1	353.5	8.54	0.07	C=O		
2	178.8	7.46	0.25	OH		
cysteine hydrochloride					this study	na
1	353.5	8.65	0.18	C=O		
2	174.9	7.41	0.27	OH		
glutamine hydrochloride					this study	53
1	319.8	8.20	0.03	C=O		
2	$306 \pm 1$	$8.30 \pm 0.1$	$0.03 \pm 0.03$			
3	$180 \pm 1$	7.75	0.24	OH		

<sup>a</sup>  $P_{\text{Q}}$  values obtained from multiple-field DAS data. <sup>b</sup> na = not available.

in the simulation both DOR, shown in Figure 2c, and 3Q MAS NMR were carried out. As can be seen DOR produces a large increase in the resolution, and two narrow lines at 228 and 218 ppm, with associated spinning sidebands, can be identified by varying the spinning speed from 1300 to 1800 Hz. The peak

position ( $\delta_{\text{peak}}$ ) in DOR spectra is given by

$$\delta_{\text{peak}} = \delta_{\text{cs,iso}} - \frac{3}{40} F(I) \frac{\chi_{\text{Q}}^2}{\nu_0^2} \left( 1 + \frac{\eta^2}{3} \right) \quad (1)$$



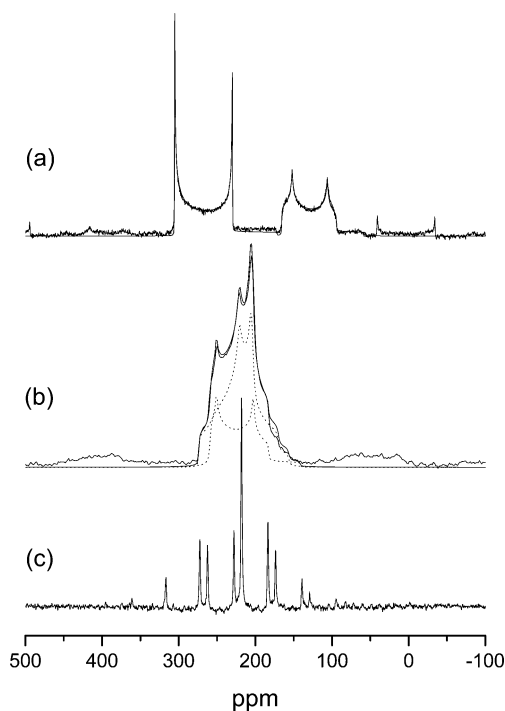


**Figure 2.** (a)  $^{17}\text{O}$  MAS NMR spectrum of L-alanine hydrochloride together with simulation, (b) MAS NMR spectrum of L-alanine together with simulation, and (c) DOR spectrum of L-alanine, outer rotor speed 1800 Hz.

where  $\delta_{\text{cs,iso}}$  is the isotropic chemical shift,  $\nu_0$  is the Larmor frequency, and  $F(I)$  is a spin-dependent factor, which for  $I = 5/2$  is  $2/25$ . Analysis at multiple applied magnetic fields<sup>1,38</sup> allows  $P_Q$  and  $\delta_{\text{cs,iso}}$  to be deduced. Alternately, if an MQ MAS experiment is carried out, one field is sufficient since in a 3Q MAS experiment the quadrupolar shift from the second term in eq 1 changes sign and is multiplied by  $10/17$ .<sup>2,39</sup> Thus, the peak position in the isotropic dimension will be that corresponding to a negative  $1/\nu_0^2$ , and plotting the center of gravity against the inverse of the square of the Larmor frequency allows both the isotropic chemical shift and, from the gradient,  $P_Q$  to be deduced. Such a plot is shown in Figure 3. Also shown on the plot are the isotropic shifts determined from the MAS simulation. The anisotropic dimension in the 3Q data clearly shows that the line with an isotropic shift of 260.5 ppm had a high  $\eta$  and that with a shift of 284 ppm a low  $\eta$ , in agreement with the MAS simulation. The values of  $\delta_{\text{cs,iso}}$ ,  $\chi_Q$ , and  $\eta$  for both forms of alanine are given in Table 1. The  $P_Q$  calculated from our  $\chi_Q$  and  $\eta$  agrees with the DAS measurements<sup>28</sup> (to within their stated error), as do the shifts. The agreement is not as good with the measurements of Wu et al. on D-alanine.<sup>30</sup> Wu et al. find both sites have a high  $\eta$  ( $0.65$  and  $0.60 \pm 0.01$ ) compared with the low  $\eta$  ( $0.28 \pm 0.03$ ) found here for the line at 284 ppm that is clearly needed to simulate the MAS spectrum. The shift of this line is also somewhat removed from the value,  $275 \pm 5$  ppm, obtained by Wu. Assignment of the two lines is less clear from the NMR parameters for L-alanine than for L-alanine hydrochloride since the chemical shift differs by only 25 ppm compared with the  $\sim 150$  ppm shift difference typical of the amino acid hydrochlorides (Table 1). The undecoupled DOR line width of the line at 218 ppm in the DOR spectrum is a little larger than that of the line at 228 ppm, indicating perhaps some residual proton coupling contribution to the line width, and in fact the line widths of both lines were found to depend strongly on the  $^1\text{H}$  decoupling field, initially increasing as the decoupling field is increased. Figure 4 shows the DOR spectrum

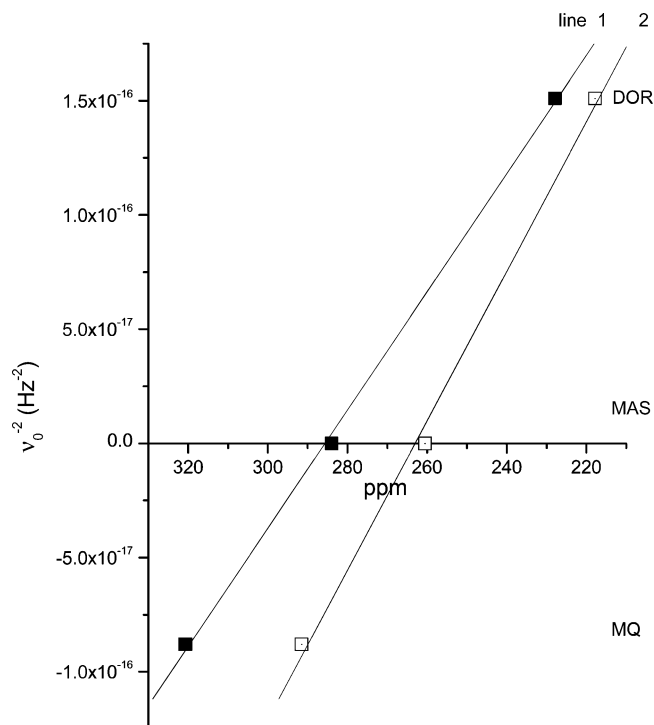


**Figure 3.** Peak position (ppm) for the two L-alanine lines as a function of the inverse square of the apparent Larmor frequency.  $\delta_{\text{cs,iso}}$  determined from the MAS simulation is also shown.

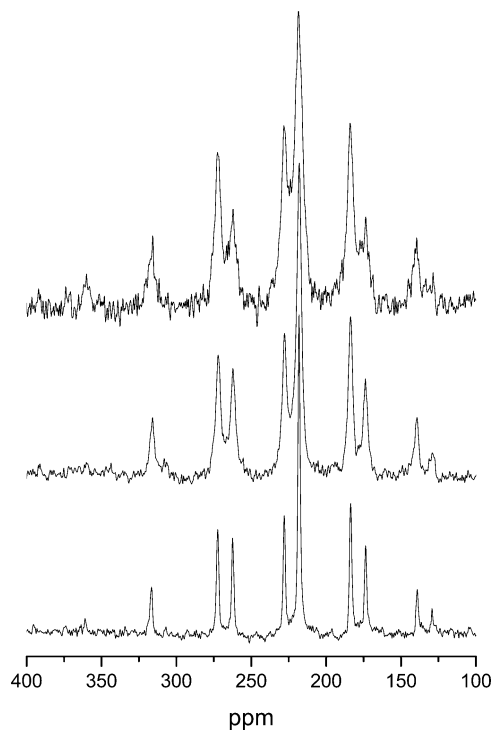


**Figure 4.** DOR spectrum of L-alanine at different  $^1\text{H}$  decoupling fields: top, decoupling 17 kHz; middle, no decoupling; bottom, decoupling 34 kHz.

with no decoupling (middle), with a decoupling field of 17 kHz (upper), and with 34 kHz decoupling (lower), and the line width as a function of decoupling field is shown in Figure 5. A maximum is seen in the line width of the 218 ppm peak which occurs at  $\sim 17$  kHz decoupling. Although the details of this are, as yet, not fully understood, it is almost certainly a rotary resonance effect<sup>40</sup> since the decoupling field is approximately twice the spinning frequency of the inner rotor (i.e.,  $\nu_{1\text{H}} = 2\nu_r$ ),

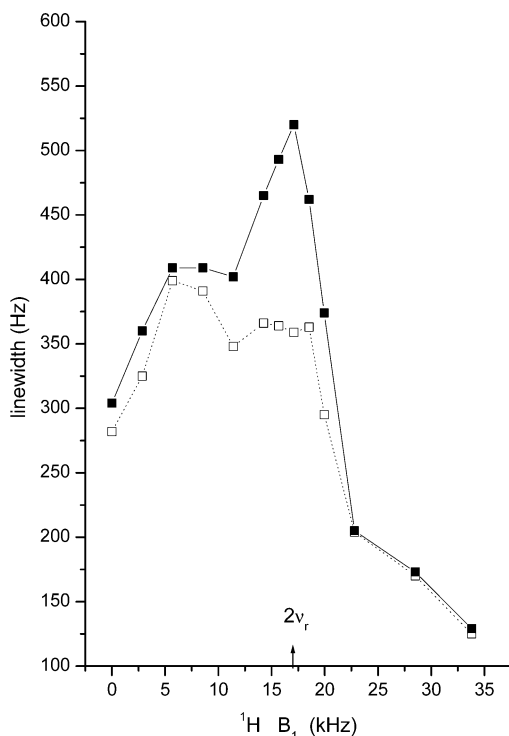


**Figure 5.** Variation of the line widths for the two lines in the DOR spectrum of L-alanine as a function of the  $^1\text{H}$  decoupling field (kHz).

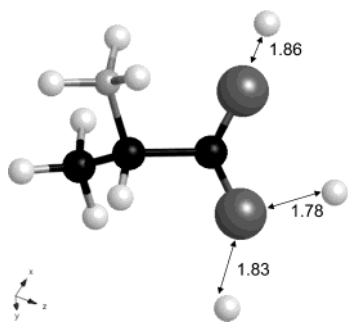


**Figure 6.** L-Alanine structure<sup>42</sup> showing the O–H distances.

which is 8.5 kHz for the outer rotor speed of 1800 Hz used here.<sup>41</sup> There is also a smaller less well delineated peak in the line width of both lines for decoupling fields of 5–10 kHz. The line at 218 ppm is approximately 50% broader at 17 kHz decoupling than that at 228 ppm, whereas at high decoupling powers their widths are similar; thus, the 218 ppm resonance experiences a significantly greater  $^1\text{H}$  dipolar coupling. The local structure around the oxygens is shown in Figure 6, and the resonances can be readily assigned, since O1 is close to one proton at 1.86 Å, whereas O2, unusually for an amino acid, has strong interaction with two protons at 1.78 and 1.83 Å.<sup>42</sup> Hence, O2 undoubtedly has the stronger dipolar coupling and corresponds to the peak at 218 ppm with an isotropic shift of 260.5 ppm. Further confirmation of the assignment is the high  $\eta$ , which is consistent with the unusual interaction with two protons. In a fashion similar to that of fmoc-protected valine the NMR parameters of fmoc-protected alanine are significantly different from those of the unprotected acid (Table 1); in particular for both protected acids the carbonyl shift is  $\sim 25$  ppm smaller than for the unprotected form.

The  $^{17}\text{O}$  MAS (Figure 7a) NMR spectrum from D-glutamic acid is more complex since the molecule has two inequivalent COOH groups so that there are two inequivalent carbonyl and hydroxyl groups in each unit cell. Hence, there are two

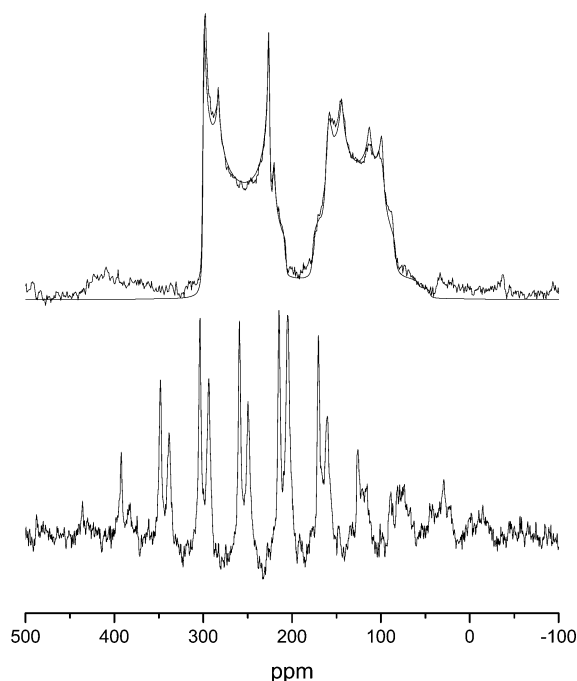


**Figure 7.**  $^{17}\text{O}$  NMR (14.1 T) spectra from D-glutamic acid hydrochloride: (a) MAS together with simulation of the centerband and (b) DOR, outer rotor speed 1800 Hz.

resonances in both the carbonyl and hydroxyl regions. Despite the extensive overlap in the MAS NMR spectrum resulting from an isotropic chemical shift difference of only  $\sim 7$  ppm for the carbonyl oxygens, a detailed simulation can be carried out that separates them completely, allowing the NMR parameters from each to be deduced (Table 1) as was discussed in detail recently for L-glutamic acid.<sup>31</sup> The two lines at lower shift come from OH oxygens (O1 and O4), and to obtain the resolution shown in Figure 7, high-power ( $> 100$  kHz)  $^1\text{H}$  decoupling was necessary. The DOR spectrum (Figure 7b) shows only two lines spaced by  $\sim 10$  ppm. There is no evidence of narrowed DOR resonances from the hydroxyls that would appear at isotropic shifts of  $\sim 135$  and 120 ppm. The maximum  $^1\text{H}$  decoupling in these DOR experiments is only 34 kHz, and the absence of the signals from the hydroxyl oxygens is attributed to the much larger  $^1\text{H}$  dipolar coupling of these oxygen sites where the protons are  $\sim 1.0$  Å away. Consequently, the lines are not narrowed by the outer rotation rate of up to 1800 Hz with the decoupling power available. As with L-alanine the differing responses of the  $^{17}\text{O}$  DOR line widths to  $^1\text{H}$  decoupling allows assignment of these two lines. The line widths of the two carbonyl oxygens with no decoupling were  $290 \pm 15$  and  $360 \pm 20$  Hz, and this already implies that the line with the larger line width is for an oxygen closer to protons. Inspection of the structure,<sup>43</sup> given in Figure 8, shows that the nearest proton to O2 is at 1.96 Å whereas the closest H to O3 is at 1.62 Å. The narrower line at  $\sim 258$  ppm in the DOR spectrum narrows by around 30% on the application of 28 kHz  $^1\text{H}$  decoupling, whereas the line width of the broader line at  $\sim 249$  ppm is still greater than the undecoupled line width. Thus, we can assign these to O2 and O3, respectively.

## Discussion

The data on the D-glutamic acid allow a direct comparison with those of the L-glutamic acid that was recently analyzed in detail.<sup>31</sup> Within error, the parameters deduced from the normal MAS spectra (which can be accurately determined because of

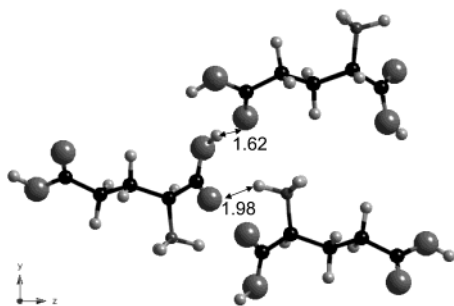


**Figure 8.** Structure of L-glutamic acid hydrochloride<sup>43</sup> showing the distance from the carbonyl atoms to the nearest proton.

the high degree of detail within the spectra) appear similar. Although DOR averages the second-order interactions, and hence some of the information that would distinguish sites is lost, the production of narrow well-resolved resonances provides further confirmation of the similarity of the NMR parameters of these samples. Despite being able to determine the position to an accuracy of  $\sim 1$  ppm, it appears that the shifts of the two carbonyl oxygens are the same in the two forms.

A rather different  $^{17}\text{O}$  NMR spectrum of glutamic acid hydrochloride was presented by Wu et al.<sup>30</sup> The spectrum was analyzed as having a line at 170 ppm with  $\chi_Q = 7.2$  MHz and  $\eta = 0.20$  and another at 320 ppm with  $\chi_Q = 8.2$  MHz and  $\eta = 0$ , with the other two sites having very similar shifts of  $\sim 250$  ppm with  $\chi_Q = 6.8$  MHz and  $\eta = 0.58$ . Although the two outer lines are at positions similar to those found for the OH sites, O1 and O4, and C=O sites, O2 and O3, respectively, the lines at 250 ppm are not observed here. Lemaitre et al.<sup>31</sup> suggested that, since the sample of Wu was enriched from D,L-glutamic acid monohydrate, it may have been racemic D,L-glutamic acid hydrochloride. (D,L-Glutamic acid monohydrate was used by Dunitz et al.<sup>44</sup> to produce racemic anhydrous D,L-glutamic acid.) Unfortunately, there is no structure in the literature for racemic D,L-glutamic acid hydrochloride, but interestingly, a recent calculation of the NMR parameters for anhydrous D,L-glutamic acid<sup>45</sup> does predict that one site, O2, will have parameters, 256 ppm, 6.8 MHz, and  $\eta = 0.72$ , similar to those of the intermediate line observed by Wu et al.

The range of  $^{17}\text{O}$  NMR parameters from the amino acid hydrochlorides shows some very interesting features (Table 1), with the OH and carbonyl oxygens showing quite clearly defined ranges of the parameters. For hydroxyls  $\chi_Q$  lies in the range 7.29–7.67 MHz and  $\delta_{\text{cs,iso}}$  varies from 172.5 to 187 ppm, while for the carbonyls  $\chi_Q$  lies in the range 8.16–8.65 MHz and  $\delta_{\text{cs,iso}}$  varies from 315 to 353.5 ppm. The asymmetry parameters are also closely defined, and are significantly different for the hydroxyl and carbonyl oxygens, indicating the differences in the bonding between these two sites. Generally, the OH sites tend to exhibit asymmetry parameters significantly removed from axial symmetry in the range 0.19–0.30, indicating that the proton is a little displaced from the line joining the oxygens. The carbonyl sites are generally close to axial symmetry, typically in the range 0.00–0.06, showing that the C=O bond is strongly defined. The O3 carboxyl site in glutamic acid has  $\eta = 0.17$ , probably because the relatively close H on the adjoining molecule (at 1.62 Å) is affecting the bonding.

Despite the quite tightly defined ranges of these parameters, the high-quality spectra that are obtained mean that the different amino acids can be readily distinguished. So, for example, mixtures of two amino acids could certainly be separated in both the MAS spectra, from the features of the second-order quadrupole line shape, and from the different net shifts (eq 1)

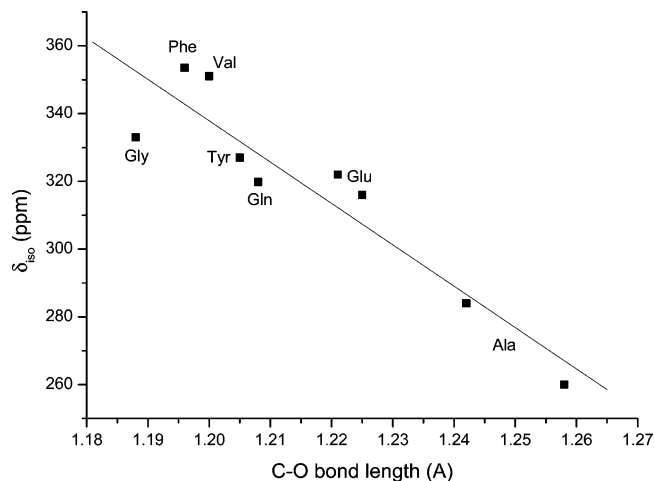


**Figure 9.** Correlation of  $\delta_{\text{cs,iso}}$  with the C–O bond length for the carbonyl oxygen in amino acids for which structural data are available.

in the DOR, producing separate resonances. As the variation of the NMR parameters between the different amino acids is much greater than the accuracy with which they can be measured, the variations can be used as a sensitive probe of the structure. One of the key steps now necessary is to further develop this probe to establish links between the NMR parameters and structural motifs. For the carbonyl oxygens there is a strong correlation ( $r = -0.93$ ) between  $\delta_{\text{cs,iso}}$  and the C–O bond length, which is shown in Figure 9. As the C–O bond length increases the shift decreases with a slope of  $\sim -1200$  ppm/Å. There is also a correlation that is not as good between the electric field gradient and C–O bond length. It is interesting that although the asymmetry parameter is close to zero for C–O distances  $\leq 1.22$  Å, with longer bond lengths it seems to increase rapidly, indicating increased hydrogen bonding.

An exciting possibility for this type of work lies in recent improvements in full electronic calculations of the NMR parameters using the gauge-included projector augmented wave method that uses pseudopotentials in a periodic structure rather than having to use a cluster approximation.<sup>46</sup> As these calculations are based on the crystal structures, they provide a direct link between the structural features and the NMR parameters. It will be shown in a separate paper that calculations of the NMR parameters are in very good agreement with the measured values.<sup>45</sup>

Another question that these experimental data allow to be addressed is the likely capability of  $^{17}\text{O}$  NMR to probe more complex biomolecules containing amino acids as building blocks. Given the highly defined line shapes, spectra made up of several different amino acids could be deconvolved under MAS. DOR also provides an important alternative since, with sufficient  $^1\text{H}$  decoupling, highly resolved spectra are obtained with line widths of only  $\sim 1$ –2 ppm. Thus, samples with many inequivalent oxygen sites could be resolved under these conditions. Also, as is common practice for  $^{13}\text{C}$  and  $^{15}\text{N}$  studies of biomolecules, site-specific  $^{17}\text{O}$  labeling could be carried out. For most samples studied here  $\leq 20$  atom % enriched  $\text{H}_2\text{O}$  was used; however, this could be increased to  $\geq 75$  atom % enrichment. This, in combination with higher magnetic fields and application of techniques that enhance the signal either by manipulation of the satellite transition populations<sup>47</sup> or possibly through the application of a train of echoes (e.g., QCPMG),<sup>48</sup> means that structurally dilute oxygen sites could be observed. It is entirely feasible that biomolecules comprising 50–100 amino acid residues enriched at one position could be observed by a combination of MAS and DOR. This capability would bring

many molecules of biological importance into the compass of solid-state  $^{17}\text{O}$  NMR.

## Conclusion

$^{17}\text{O}$  NMR data can be readily collected at reasonably high fields (14.1 T) from amino acids with good signal-to-noise ratios from samples where only 10–20 atom %  $^{17}\text{O}$  enriched water was used in the sample preparation. Typical  $^{17}\text{O}$  MAS NMR spectra consist of well-separated second-order quadrupole line shapes from the carbonyl and hydroxyl oxygens. The highly detailed MAS centerbands obtained mean that the NMR parameters can be accurately deduced and variations between the different amino acids readily determined. DOR produces significant additional narrowing over the MAS spectra, typically a factor  $\sim 40$ , so that high-resolution spectra with line widths of  $\sim 1$  ppm are obtained. A combination of MAS, DOR, and 3Q MAS can provide a high accuracy of the NMR parameters, even for samples for which there is significant overlap between the different resonances in the MAS NMR spectra. L-Alanine shows a spectrum very different from those of the amino acid hydrochlorides because of the very different bonding arrangements at the different oxygen sites in the two forms. Variation of the DOR line width with  $^1\text{H}$  decoupling power allows the assignment of different carbonyls because of their differing spatial proximity to the protons. Decoupling powers significantly greater than the 34 kHz used here will be necessary to narrow the  $^{17}\text{O}$  resonances from hydroxyl oxygens under DOR. A strong correlation is observed between the chemical shift  $\delta_{\text{CS,iso}}$  and the C–O bond length so that  $^{17}\text{O}$  has significant potential to provide new information about bonding in these systems. The sensitivity and resolution obtained provide much optimism that  $^{17}\text{O}$  NMR data could usefully be collected from much larger biomolecules, for example, to provide information about site-specific binding and receptor–ligand interactions.

**Acknowledgment.** The EPSRC is thanked for supporting the NMR equipment at Warwick and the work on biological materials through Grant GR/N29549. The Royal Society has supported the collaboration with Tallinn, Estonia, and M.E.S. also thanks the Royal Society and Leverhulme Trust for the award of a Senior Research Fellowship 2001–2002 under which some of this work was carried out. A.W. and V.L. thank BBSRC and Nestec for support, and Dr. E. Hughes for advice. The Estonian Science Foundation is also thanked for support, and Dr. S. P. Brown is thanked for collecting the  $^{13}\text{C}$  CP MAS NMR data on the alanine samples.

## References and Notes

- (1) Smith, M. E.; van Eck, E. R. H. *Prog. NMR Spectrosc.* **1999**, *34*, 154.
- (2) MacKenzie, K. J. D.; Smith, M. E. *Multinuclear Solid State NMR of Inorganic Materials*; Pergamon Press: Oxford, 2002.
- (3) Dirken, P. J.; Smith, M. E.; Whitfield, H. J. *J. Phys. Chem.* **1995**, *99*, 395.
- (4) Pickup, D. M.; Mountjoy, G.; Wallidge, G. W.; Anderson, R.; Cole, J. M.; Newport, R. J.; Smith, M. E. *J. Mater. Chem.* **1999**, *9*, 1299.
- (5) Gervais, C.; Babonneau, F.; Smith, M. E. *J. Phys. Chem. B* **2001**, *105*, 1971.
- (6) Dirken, P. J.; Kohn, S. C.; Smith, M. E.; van Eck, E. R. H. *Chem. Phys. Lett.* **1997**, *266*, 568.
- (7) Hussin, R.; Dupree, R.; Holland, D. *J. Non-Cryst. Solids* **1999**, *246*, 159.
- (8) Zhao, P. D.; Kroeker, S.; Stebbins, J. F. *J. Non-Cryst. Solids* **2000**, *276*, 122.
- (9) Stebbins, J. F.; Zhao, P. D.; Lee, S. K.; Oglesby, J. V. *J. Non-Cryst. Solids* **2001**, *293*, 67.
- (10) Bull, L. M.; Bussemer, B.; Anupold, T.; Reinhold, A.; Samoson, A.; Sauer, J.; Cheetham, A. K.; Dupree, R. *J. Am. Chem. Soc.* **2000**, *122*, 4948.
- (11) Pingel, U. T.; Amoureux, J.-P.; Anupold, T.; Bauer, F.; Ernst, H.; Fernandez, C.; Freude, D.; Samoson, A. *Chem. Phys. Lett.* **1998**, *294*, 345.
- (12) Kroeker, S.; Rice, D.; Stebbins, J. F. *Am. Mineral.* **2002**, *87*, 572.
- (13) Ashbrook, S. E.; Berry, A. J.; Wimperis, S. *J. Am. Chem. Soc.* **2001**, *125*, 6360.
- (14) Watts, A. *Curr. Opin. Biotechnol.* **1999**, *10*, 48.
- (15) Watts, A. *Pharm. Pharmacol. Commun.* **1999**, *5*, 7.
- (16) Godbout, N.; Sanders, L. K.; Salzman, R.; Halvon, R. H.; Wojdelski, M.; Oldfield, E. *J. Am. Chem. Soc.* **1999**, *121*, 3829.
- (17) Howes, A. P.; Jenkins, R.; Smith, M. E.; Crout, D. H. G.; Dupree, R. *Chem. Commun.* **2001**, 1448.
- (18) Wu, G.; Dong, S.; Ida, R.; Reen, N. *J. Am. Chem. Soc.* **2002**, *124*, 1768.
- (19) Dong, S.; Yamada, K.; Wu, G. *Z. Naturforsch.* **2000**, *55A*, 21.
- (20) Steinschneider, A.; Burgar, M. I.; Buku, A.; Fiat, D. *Int. J. Pept. Protein Res.* **1981**, *18*, 324.
- (21) Steinschneider, A.; Valentine, B.; Burgar, M. I.; Fiat, D. *Magn. Reson. Chem.* **1985**, *23*, 104.
- (22) Goc, R.; Ponnusamy, E.; Tritt-Goc, J.; Fiat, D. *Int. J. Pept. Protein Res.* **1988**, *31*, 130.
- (23) Goc, R.; Tritt-Goc, J.; Fiat, D. *Bull. Magn. Reson.* **1989**, *11*, 238.
- (24) Kuroki, S.; Ando, I.; Shoji, A.; Ozaki, T. *J. Chem. Soc., Chem. Commun.* **1992**, 433.
- (25) Kuroki, S.; Takahashi, A.; Ando, I.; Shoji, A.; Ozaki, T. *J. Mol. Struct.* **1994**, *323*, 197.
- (26) Yamauchi, K.; Kuroki, S.; Ando, I. *J. Mol. Struct.* **2002**, *602–603*, 171.
- (27) Seliger, J.; Zagar, V.; Blinc, R.; Kadaba, P. K.; Fiat, D. *Z. Naturforsch.* **1990**, *45A*, 733.
- (28) Yamauchi, K.; Kuroki, S.; Ando, I.; Ozaki, T.; Shoji, A. *Chem. Phys. Lett.* **1999**, *302*, 331.
- (29) Gann, S. L.; Baltisberger, J. H.; Wooten, E. W.; Zimmermann, H.; Pines, A. *Bull. Magn. Reson.* **1994**, *16*, 68.
- (30) Wu, G.; Dong, S. *J. Am. Chem. Soc.* **2001**, *123*, 9119.
- (31) Lemaitre, V.; Pike, K. J.; Watts, A.; Anupold, T.; Samoson, A.; Smith, M. E.; Dupree, R. *Chem. Phys. Lett.* **2003**, *371*, 91.
- (32) Torrent, M.; Mansour, D.; Day, E. P.; Morokuma, K. *J. Phys. Chem. A* **2001**, *105*, 4546.
- (33) Torres, J.; Kukol, A.; Arkin, I. T. *Biopolymers* **2001**, *59*, 396.
- (34) Kunwar, A. C.; Turner, G. L.; Oldfield, E. *J. Magn. Reson.* **1986**, *69*, 124.
- (35) Detken, A.; Hardy, E. H.; Ernst, M.; Meier, B. H. *Chem. Phys. Lett.* **2002**, *356*, 298.
- (36) Samoson, A.; Lippmaa, E. *J. Magn. Reson.* **1989**, *84*, 410.
- (37) Massiot, D.; Fayon, F.; Capron, M.; King, I.; Le Calvi, S.; Alonso, B.; Durand, J.-O.; Bujoli, B.; Gan, Z.; Hoatson, G. *Magn. Reson. Chem.* **2002**, *40*, 70.
- (38) Anupold, T.; Reinhold, A.; Sarv, P.; Samoson, A. *Solid State NMR* **1998**, *13*, 87.
- (39) Pike, K. J.; Malde, R. P.; Ashbrook, S. E.; Mcmanus, J.; Wimperis, S. *Solid State NMR* **2000**, *16*, 203.
- (40) Wi, S.; Logan, J. W.; Sakellariou, D.; Walls, J. D.; Pines, A. *J. Chem. Phys.* **2002**, *117*, 7024.
- (41) Wu, Y.; Sun, B. Q.; Pines, A.; Samoson, A.; Lippmaa, E. *J. Magn. Reson.* **1990**, *89*, 297.
- (42) Lehmann, M. S.; Koetzle, T. F.; Hamilton, W. C. *J. Am. Chem. Soc.* **1972**, *94*, 2657.
- (43) Sequeira, A.; Rajagopal, H.; Chidambaram, R. *Acta Crystallogr., B* **1972**, *28*, 2514.
- (44) Dunitz, J. D.; Schweizer, W. B. *Acta Crystallogr., C* **1995**, *51*, 1377.
- (45) Yates, J. R.; Pickard, C. J.; Payne, M. C.; Dupree, R.; Profeta, M.; Mauri, F. *J. Phys. Chem. B*, in press.
- (46) Pickard, C.; Mauri, F. *Phys. Rev. B* **2001**, *245101*.
- (47) Madhu, P. K.; Pike, K. J.; Dupree, R.; Levitt, M. H.; Smith, M. E. *Chem. Phys. Lett.* **2003**, *367*, 150.
- (48) Larsen, F. H.; Farnan, I. *Chem. Phys. Lett.* **2002**, *357*, 403.
- (49) di Blasio, B.; Pavone, V.; Pedone, C. *Cryst. Struct. Commun.* **1977**, *6*, 745.
- (50) Frey, M. N.; Koetzle, T. F.; Lehmann, M. S.; Hamilton, W. C. *J. Chem. Phys.* **1973**, *58*, 2547.
- (51) Koetzle, T. F.; Golic, L.; Lehmann, M. S.; Verbist, J. J.; Hamilton, W. C. *J. Chem. Phys.* **1974**, *60*, 4690.
- (52) Al-Karaghoul, A. R.; Koetzle, T. F. *Acta Crystallogr., B* **1975**, *31*, 2461.
- (53) Shamala, N.; Venkatesan, K. *Cryst. Struct. Commun.* **1972**, *1*, 227.